

Review

A theoretical method to analyze the glass–crystal transformation kinetics under non-isothermal regime: Application to crystallization of the $\text{Ge}_{0.13}\text{Sb}_{0.23}\text{Se}_{0.64}$ glassy alloy

J. Vázquez*, D. García-G.Barreda, J.L. Cárdenas-Leal, P.L. López-Alemaný, P. Villares, R. Jiménez-Garay

Departamento de Física de la Materia Condensada, Facultad de Ciencias, Universidad de Cádiz, Apartado 40, 11510 Puerto Real, Cádiz, Spain

ARTICLE INFO

Article history:

Received 14 April 2008

Received in revised form

10 June 2008

Accepted 23 July 2008

PACS:

61.40

64.60.Qb

64.70.Kb

64.70.Pf

Keywords:

Glassy alloy

Glass–crystal transformation

Reaction mechanism

Temperature integral

Differential scanning calorimetry

Kinetic parameters

ABSTRACT

A theoretical method has been considered to determine the suitable form of the glass–crystal transformation function, and to calculate the kinetic parameters by using differential scanning calorimetry data, obtained from experiments carried out under non-isothermal regime. It is an integral method, which is based on a transformation rate independent of the thermal history and expressed as the product of two separable functions of absolute temperature and the volume fraction transformed. Considering the same temperatures for the different heating rates, one obtains a constant value for temperature integral, and therefore a plot of a function of the volume fraction transformed versus the reciprocal of the heating rate leads to a straight line with an intercept of zero, if the reaction mechanism is correctly chosen. Besides, by using the first mean value theorem to approach the temperature integral, one obtains a relationship between a function of the temperature and other function of the volume fraction transformed. The logarithmic form of the quoted relationships leads to a straight line, whose slope and intercept allow to obtain the activation energy and the frequency factor, respectively. The theoretical method has been applied to the crystallization kinetics of the $\text{Ge}_{0.13}\text{Sb}_{0.23}\text{Se}_{0.64}$ glassy alloy and it has been found that the kinetic model of normal grain growth is most suitable to describe the crystallization of the quoted alloy. The values obtained for the activation energy, E , and the logarithm of the frequency factor, K_0 , have been $188.3 \text{ kJ mol}^{-1}$ and 36.7 (K_0 in s^{-1}), respectively. The phases at which the alloy crystallizes after the thermal process have been identified by X-ray diffraction. The diffractogram of the transformed material suggests the presence of microcrystallites of Sb_2Se_3 and GeSe , remaining in a residual amorphous matrix.

© 2008 Elsevier B.V. All rights reserved.

Contents

1. Introduction	3958
2. Theoretical background	3958
2.1. Applicability of the JMA equation under non-isothermal regime	3959
2.2. Calculating kinetic parameters	3959
3. Experimental details	3960
4. Results	3960
4.1. Glass–crystal transformation	3960
5. Identification of the crystalline phases	3962
6. Conclusions	3962
Acknowledgements	3963
References	3963

* Corresponding author.

E-mail address: jose.vazquez@uca.es (J. Vázquez).

1. Introduction

The glass–crystal transformation has been studied intensively by the researchers of the last six decades, especially since Duwez et al. [1] published their introduction to the preparation of glassy alloys by quenching technique. These materials have received great attention in the past 50 years due to their unique isotropic, structural and chemical properties [2,3]. An understanding of the kinetics of crystallization in glasses is important for the manufacturing of glass–ceramics and in preventing devitrification. Differential scanning calorimetry (DSC) is valuable for the quantitative study of crystallization in different glassy systems. This study of crystallization kinetics has been widely discussed in the literature [4–7] during the last half century. Thus, it is well-known that the theoretical basis for interpreting DSC results is provided by the formal theory of transformation kinetics as developed by Johnson–Mehl–Avrami (JMA) [8–10], which is a completely general theory and which has been originally derived for non-isothermal conditions as well as for isothermal. In the case of isothermal crystallization with nucleation frequency and growth rate independent of time, the JMA general expression can be easily integrated, giving a straightforward equation. It should be noted, however, that the quoted equation strictly applies only to isothermal experiments [11]. Nevertheless, many authors have used the above-mentioned equation to derive expressions describing non-isothermal transformations [12,13]. This fact shows an incomplete understanding of the formal theory of transformation kinetics, as Henderson has suggested in a notable work [14].

In this work, a theoretical method is considered to determine the most adequate form of the transformation function, $f(x)$, and to calculate the kinetic parameters: activation energy and frequency factor, by using DSC data obtained from experiments carried out with different heating rates. The quoted method assumes that the reaction rate depends only on the volume fraction transformed and temperature, and that these variables are independent ones [15,16]. In addition, the present work applies the above-mentioned method to the analysis of the crystallization kinetics of the $\text{Ge}_{0.13}\text{Sb}_{0.23}\text{Se}_{0.64}$ glassy semiconductor and the results obtained reveal that the quoted crystallization does not fulfil correctly the JMA model. However, it seems that the kinetic model of normal grain growth, R_n , is the most adequate to describe the crystallization of the glass studied.

2. Theoretical background

The main finality of the kinetic analysis of a glass–crystal transformation under non-isothermal regime is the determination of the corresponding parameters: activation energy, E , kinetic exponent, n , and frequency factor, K_0 , in addition to the analytical form of the transformation function $f(x)$. It is well-known that the methods used to evaluate the quoted parameters are usually classified as differential and integral methods [15]. Both types of methods may be classified further as being based on data acquired

for one or more heating rates. It is considered that an integral method based on data recorded for various heating rates could give results which are more reliable and less affected by errors, since the quoted method evaluates the whole experimental data set and it is based on the primary experimentally acquired data, x and T . The integral method proposed in this work assumes, as in most solid-state transformations, that the reaction rate, dx/dt , for thermal treatments under non-isothermal regime can be expressed as a product of two separable functions of absolute temperature, T , and the volume fraction transformed, x [16]

$$dx/dt = K(T)f(x) \quad (1)$$

where $K(T)$ is the reaction rate constant and $f(x)$ a function of x and reflects the mechanism of transformation.

Some authors [17] introduce two further requirements: that $f(x)$ is independent of the heating rate, β , and that the temperature dependence of the reaction rate constant, K , is exponential, Arrhenius type, $K(T) = K_0 \exp(-E/RT)$, which allows to calculate the activation energy.

In accordance with the literature [15], by integrating Eq. (1) with the usual change of the variable time into temperature, one obtains

$$F_{rs} = \int_{x_r}^{x_s} \frac{dx}{f(x)} = \frac{1}{\beta} \int_{T_r}^{T_s} K(T) dT = \frac{1}{\beta} I_{rs} \quad (2)$$

where x_r , x_s are two different degrees of conversion, T_r , T_s are their corresponding temperatures, and it is considered a heating rate $\beta = dT/dt$.

It should be noted that by means of Eq. (2) different values of $F(x)$ function are obtained from the same temperature intervals using DSC scans at different heating rates. Consequently, it is assumed that the kinetic parameters are independent of the crystallized volume fraction and that the values obtained for the quoted parameters are just the averages over the transformation. Once the above considerations are assumed, for two selected temperatures T_r and T_s , one can determine pairs of values of x , i.e., (x_{r1}, x_{s1}) , (x_{r2}, x_{s2}) ,... for the experimental data at different heating rates. From these pairs and using various kinetic model functions, such as those given in Table 1, the values of F_{rs1} , F_{rs2} ,... can be calculated according to Eq. (2). As the temperatures T_r and T_s are the same for all the experiments, considering again Eq. (2), it follows that I_{rs} is constant, and therefore the plots of the values of F_{rs} versus $1/\beta$ have to lead to a straight line with an intercept of zero, if the analytical form of $f(x)$ is correctly chosen. The procedure may be repeated for other pairs of temperatures and, consequently, other straight lines will be obtained for the correct form of $f(x)$, by using the best correlation coefficient to choose the suitable kinetic model function. Nevertheless, it is well-known that for the crystallization of glassy alloys, the experimental DSC data are generally analyzed with the framework of formal theory of nucleation and growth, and then the mostly used expression of $f(x)$ is the JMA equation [8–10] (Table 1) with n called kinetic exponent.

Table 1
Theoretical kinetic model equations considered

Model	$f(x)$	$F(x)$	Label
Johnson–Mehl–Avrami (JMA)	$n(1-x)[- \ln(1-x)]^{(n-1)/n}$	$[- \ln(1-x)]^{1/n}$	A_n
Three-dimensional diffusion	$3/2[(1-x)^{-1/3} - 1]^{-1}$	$1 - (2/3)x - (1-x)^{2/3}$	D
Mampel unimolecular law, $n = 1$	$1-x$	$- \ln(1-x)$	R_1
Normal grain growth	$(1-x)^n$	$[1 - (1-x)^{1-n}]/(1-n)$	R_n

2.1. Applicability of the JMA equation under non-isothermal regime

The JMA equation was originally adapted to analyze isothermal DSC data. Henderson [5,14] and De Bruijn et al. [6] have shown that the validity of the quoted equation can be extended in non-isothermal regime if the entire nucleation process takes place during the early stages of the transformation, and it becomes negligible afterward. This case has been referred to as “site saturation” in the literature [18]. Thus, it seems necessary to develop a simple and reliable method to test the applicability of the JMA equation. In this sense, we define the functions $y(x)$ and $z(x)$ that can be easily obtained by a simple transformation of experimental data. The quoted functions are proportional to the $f(x)$ and $f(x)F(x) = f(x) \int_0^x dx'/f(x')$ functions, respectively, which are invariant with respect to the experimental variables.

When the continuous heating regime is used, it is necessary to define $y(x) = (\Delta H_c)(dx/dt)\exp(E/RT)$, with ΔH_c the total enthalpy change associated with the transformation, and considering Eq. (1), one obtains

$$y(x) = A_1 f(x) \tag{3}$$

where $A_1 = (\Delta H_c) K_0$ is a constant.

In the case of $z(x)$ function, by using the substitution $u' = E/RT$, the temperature integral $\int_{T_0}^T K(T')dT'$, Eq. (2), is transformed in an exponential integral of order two, which can be expressed, in accordance with the literature [19], by an alternating series, and Eq. (2) in the interval of transformed volume fraction ($0 \leq x' \leq x$) becomes

$$F(x) = \frac{K_0 E}{\beta R} \left[\frac{e^{-u}}{u^2} \sum_{k=0}^{\infty} \frac{(-1)^k (k+1)!}{u^k} \right]_{u_0}^u \tag{4}$$

Given that $T > T_0$ (T_0 is the starting temperature) and, therefore, $u_0 = qu$ with $q > 1$, Eq. (4) can be expressed as

$$F(x) = \frac{K_0 E e^{-u}}{\beta R u^2} \sum_{k=0}^{\infty} \frac{(-1)^k (k+1)!}{u^k} (1-Q) \quad \text{with} \tag{5}$$

$$Q = \frac{1}{q^2} e^{-(q-1)u} \frac{\sum_{k=0}^{\infty} (-1)^k (k+1)! / q^k u^k}{\sum_{k=0}^{\infty} (-1)^k (k+1)! / u^k}$$

Bearing in mind that in most glass–crystal transformation $u = E/RT \gg 1$, usually $E/RT \geq 25$ [11] the exponential function $e^{-(q-1)u} \ll 1$. Moreover, it should be noted that, in practice, the quoted temperatures T and T_0 do not differ by more than 5–10%, in accordance with the literature [13] and it be verified that, in the worse case (difference of 10%), the quotient of the series in the Q function is approximately 1. Accordingly, the quoted Q function is negligible in comparison with the unit, and Eq. (5) becomes

$$F(x) = \frac{K_0 E e^{-u}}{\beta R u^2} \sum_{k=0}^{\infty} \frac{(-1)^k (k+1)!}{u^k} \tag{6}$$

$$= \frac{K_0 T}{\beta} \left[\exp\left(\frac{-E}{RT}\right) \right] S\left(\frac{E}{RT}\right)$$

where the function $S(E/RT)$ is defined as $S(u) = S(E/RT) = (1/u) \sum_{k=0}^{\infty} [(-1)^k (k+1)! / u^k]$.

Next, we define the $z(x) = (\Delta H_c) T^2 (dx/dt)$ function and bearing in mind Eqs. (1) and (6), one obtains

$$z(x) = A_2 f(x) F(x) \tag{7}$$

and considering again the assumption $E/RT \geq 25$ [11], it is possible to use only the first term of the series of Eq. (6), and the approximation $S(E/RT) \approx RT/E$ is sufficiently accurate. It should be noted that $A_2 = (\Delta H_c) \beta E/R$ is a constant.

From Eqs. (3) and (7) invariant with respect to the experimental variables it can be obtained a reliable test of applicability of the JMA model. Thus, considering for the quoted model the

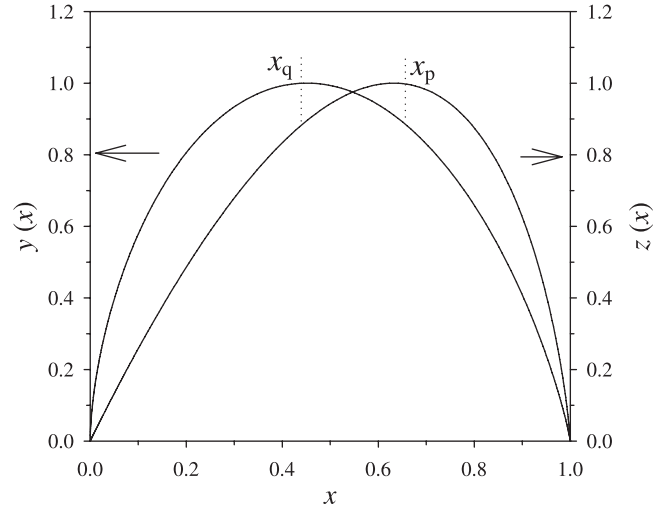


Fig. 1. Normalized $y(x)$ and $z(x)$ functions obtained from the theoretical JMA model with kinetic exponent, $n = 2.5$. The broken lines show the theoretical x_q and x_p values corresponding to the quoted model.

corresponding $f(x)$ function, given in Table 1, taking the derivative of Eq. (3) with respect to x and equalling to zero the resulting expression leads to

$$\left. \frac{df(x)}{dx} \right|_{x_q} = [-\ln(1-x_q)]^{(n-1)/n} - \frac{n-1}{n} [-\ln(1-x)]^{-1/n} = 0 \tag{8}$$

This equation allows to obtain an expression of x_q , which depends on the kinetic exponent

$$x_q = 0 \quad \text{for } n \leq 1$$

$$x_q = 1 - \exp[-(n-1)/n] \quad \text{for } n > 1 \tag{9}$$

and gives a maximum value for the $y(x)$ function.

In the case of the $z(x)$ function, taking the derivative of Eq. (7) with respect to x and setting the resulting expression equal to zero yields

$$\left. \frac{df(x)}{dx} \right|_{x_p} F(x_p) + 1 = 0 \tag{10}$$

the condition that must be fulfilled by x_p at the maximum of the $z(x)$ function.

Introducing into Eq. (10) the functions $f(x)$, and $F(x) = \int_0^x dx'/f(x')$, taken from the JMA model one obtains

$$\ln(1-x_p) = -1, \quad \text{i.e., } x_p = 0.632 \tag{11}$$

the value of the volume fraction transformed, which gives a maximum value for the $z(x)$ function. This value is a characteristic of the quoted model, and, accordingly, it can be used as a simple test of its applicability [16]. Both $y(x)$ and $z(x)$ functions are usually normalized within the (0,1) range, as it is shown in Fig. 1 for the JMA model with kinetic exponent $n = 2.5$.

2.2. Calculating kinetic parameters

Once by means of Eq. (2) it is possible to find the most probable kinetic mechanism of the studied transformation, it is necessary to calculate the values of the kinetic parameters E and K_0 [15]. Assuming an Arrhenian temperature dependence for $K(T)$ in Eq. (2), the simplest approach of I_{rs} is to use the first mean value theorem for definite integrals, obtaining

$$\int_{T_r}^{T_s} \left[\exp\left(\frac{-E}{RT}\right) \right] dT = (T_s - T_r) \exp\left(\frac{-E}{RT}\right) \tag{12}$$

where \bar{T} belongs to the (T_r, T_s) range, and accordingly, the logarithmic form of Eq. (2) can be written as

$$\ln \frac{\beta}{T_s - T_r} = \ln \frac{K_0}{F_{rs}} - \frac{E}{R\bar{T}} \quad (13)$$

For two selected volume fraction transformed x_r and x_s , one can determine a pair of values of T , i.e., (T_{ri}, T_{si}) corresponding to each β_i value. The plot of $\ln[\beta/(T_s - T_r)]$ versus $1/\bar{T}$ leads to a straight line whose slope, $-E/R$, and intercept, $\ln(K_0/F_{rs})$, allow the calculation of E and K_0 , respectively. The procedure may be repeated for other pairs of transformed fraction and, consequently, other straight lines are obtained.

3. Experimental details

The $\text{Ge}_{0.13}\text{Sb}_{0.23}\text{Se}_{0.64}$ glassy alloy was prepared in our laboratory in bulk form, by the standard melt quenching method. The components of the quoted alloy, with a purity of 99.999%, were pulverized to less than $64\ \mu\text{m}$, mixed in adequate proportions and introduced into a quartz ampoule. The content of the quoted ampoule was sealed under a vacuum of $10^{-2}\ \text{Pa}$, heated in a rotating furnace at around $1225\ \text{K}$ for $72\ \text{h}$ and then quenched in water with ice to avoid crystallization. The amorphous state of the material was confirmed by a diffractometric X-ray scan in a Siemens D500 diffractometer. The homogeneity and composition of the samples were verified through scanning electron microscopy (SEM) in a JEOL, scanning microscope JSM 820. The calorimetric measurements were carried out in a Perkin-Elmer DSC7 with an accuracy of $\pm 0.1\ \text{K}$. The samples weighing about $20\ \text{mg}$ were crimped in aluminum pans, and scanned at room temperature through their glass transition temperature, T_g , at different heating rates of 2, 4, 8, 16, 32 and $64\ \text{K}\ \text{min}^{-1}$. An empty aluminum pan was used as reference, and in all cases, a constant $60\ \text{ml}\ \text{min}^{-1}$ flow of nitrogen was maintained in order to provide a constant thermal blanket within the DSC cell, thus eliminating thermal gradients and ensuring the validity of the applied calibration standard from sample-to-sample. The glass transition temperature was considered as a temperature corresponding to the inflection of the lambda-like trace on the DSC scan, as shown in Fig. 2. With the aim of explaining clearly in this section whether all the volume of glass crystallize or not, we have introduced in this work a final section where the possible crystalline phases are identified. The diffractogram of the crystallized material shows the detected crystalline phases together with a residual amor-

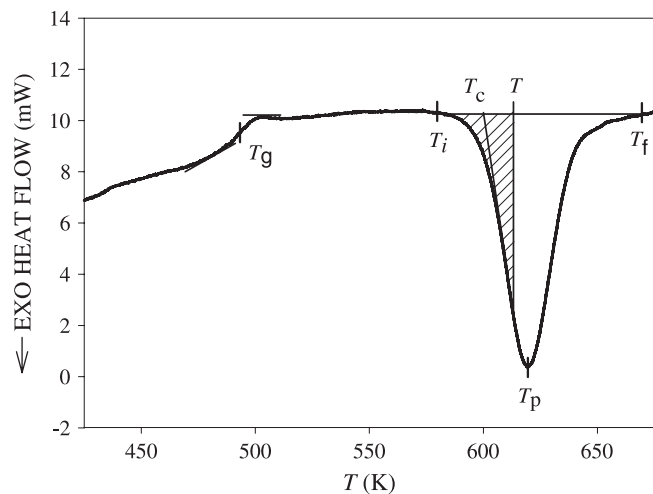


Fig. 2. Typical DSC trace of $\text{Ge}_{0.13}\text{Sb}_{0.23}\text{Se}_{0.64}$ glassy alloy at a heating rate of $32\ \text{K}\ \text{min}^{-1}$. The hatched area shows the area between T_i and T .

phous matrix (see Section 5). Maybe this glassy remainder can explain the observed deviation from the Avrami model of the experimental data corresponding to the glass–crystal transformation of the $\text{Ge}_{0.13}\text{Sb}_{0.23}\text{Se}_{0.64}$ glassy alloy.

4. Results

The typical DSC trace of $\text{Ge}_{0.13}\text{Sb}_{0.23}\text{Se}_{0.64}$ semiconductor glass obtained at $\beta = 32\ \text{K}\ \text{min}^{-1}$ and plotted in Fig. 2 shows three characteristic phenomena which are resolved in the temperature region studied. The first one ($T = 493.3\ \text{K}$) corresponds to the glass transition temperature, T_g , the second one ($T = 601.6\ \text{K}$) to the extrapolated onset crystallization temperature, T_c , and the last one ($T = 618.3\ \text{K}$) to the peak temperature of crystallization, T_p , of the quoted semiconductor glass. It should be noted that the DSC data for the different heating rates, quoted in Section 3, show values of the quantities T_g , T_c and T_p which increase with increasing β , a property which has been reported in the literature [4,20,21].

The analysis of the glass–crystal transformation kinetics of the quoted semiconductor involves to know the experimental values of the quantities, which are obtained from the thermograms corresponding to the heating rates, quoted in Section 3. The values of the mentioned quantities are given in Table 2, where T_i and T_p are the temperatures at which transformation begins and that corresponding to the maximum transformation rate, respectively, and ΔT is the width of the peak of the DSC trace. The crystallization enthalpy, ΔH , is also obtained for each of the heating rates. The area limited by the peak of the DSC trace is directly proportional to the total amount of crystallized material. The volume fraction transformed, x , at any temperature, T , is given by $x = A_T/A$, where A is the total area limited by the exotherm of the peak between the temperature, T_i , where the crystallization just begins and the temperature, T_f , where the crystallization is completed and A_T is the area between the initial temperature and a generic temperature T , (see Fig. 2). The quotients between the ordinates of the peak of the DSC curve and the total area of the same give the corresponding crystallization rates, which allow to plot the curves of dx/dt versus T for the different heating rates represented in Fig. 3. It should be noted that the values of the quantity $(dx/dt)_p$ increase in the same proportion as the heating rates, a property which has been widely discussed in the literature [20,21].

4.1. Glass–crystal transformation

The developed theory in preceding sections has been applied to the glass–crystal transformation of the $\text{Ge}_{0.13}\text{Sb}_{0.23}\text{Se}_{0.64}$ glassy semiconductor. Accordingly, to choose the most adequate kinetic mechanism, we show in Table 3 the temperatures T_p , T_s and the corresponding volume fractions transformed, at the different heating rates quoted in Section 3. With the help of the functions of Table 1 and by using the least squares method, Table 4 was

Table 2

Characteristic temperatures and enthalpies of the crystallization processes of the $\text{Ge}_{0.13}\text{Sb}_{0.23}\text{Se}_{0.64}$ alloy

Quantity	Experimental value, $\beta(\text{K}\ \text{min}^{-1})$					
	2	4	8	16	32	64
T_g (K)	474.0	478.0	481.3	494.2	495.3	499.2
T_i (K)	558.7	564.5	570.9	576.5	584.4	599.7
T_p (K)	581.1	588.0	597.5	607.7	618.3	631.3
ΔT (K)	42.2	43.0	47.5	50.1	60.2	56.7
ΔH (mJ mg $^{-1}$)	32.0	29.8	30.7	25.7	31.9	26.4

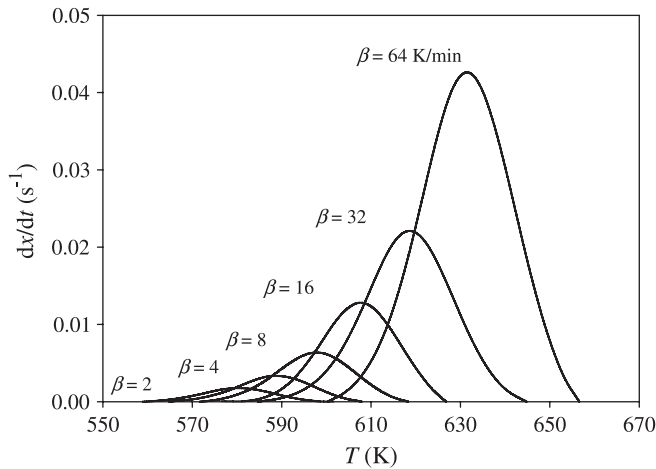


Fig. 3. Crystallization rate versus temperature of the exothermal peaks at different heating rates.

Table 3
Volume fraction transformed corresponding to various temperatures T_r , T_s at different heating rates

$T(K)$	β ($K\text{min}^{-1}$)					
	2	4	8	16	32	64
586	0.78292	0.38514	0.09168	0.00427	–	–
592	0.95280	0.67019	0.26311	0.03484	0.00438	–
602	–	0.97180	0.70939	0.26672	0.04969	0.00022
608	–	–	0.90830	0.53357	0.14471	0.00901

Table 4
Correlation coefficients corresponding to kinetic mechanisms of Table 1 for the $\text{Ge}_{0.13}\text{Sb}_{0.23}\text{Se}_{0.64}$ glassy alloy

Mechanism label	$T_r = 586\text{ K}$	$T_r = 592\text{ K}$	$T_r = 602\text{ K}$
	$T_s = 592\text{ K}$	$T_s = 602\text{ K}$	$T_s = 608\text{ K}$
A_2	0.9639	0.9734	0.9699
A_3	0.8252	0.8653	0.8384
D	0.9874	0.9825	0.9730
R_1	0.9073	0.9007	0.9140
$R_{2.2}$	0.9916	0.9877	0.9866

obtained, where the correlation coefficients for each plot of F_{rs} versus $1/\beta$ are given. The quoted coefficients are calculated for the straight lines which pass through the computed points ($1/\beta$, F_{rs}) and the origin of the axes, because as it has been already mentioned, the intercept of the plot has to be zero. It should be noted that the best correlation coefficients are obtained for the kinetic model R_n with $n = 2.2$ in accordance with Table 4. The same result was obtained for all cases which, for the sake of simplicity, are not listed in this work. Next, to calculate the kinetic parameters E and K_0 , we have chosen the volume fractions transformed and the corresponding temperatures for each β , which are given in Table 5. According to Eq. (13), the plots of $\ln[\beta/(T_s - T_r)]$ versus $1/T$ lead to straight lines whose slopes and intercepts provide the mean values: $E = 188.3\text{ kJ mol}^{-1}$ and $\ln K_0 = 36.7$ (K_0 in s^{-1}), respectively.

On the other hand, we have used the applicability test of the JMA model considering the functions: $y(x) \propto (dx/dt)\exp(E/RT)$ and $z(x) \propto T^2(dx/dt)$. The quoted normalized functions corresponding

Table 5
Temperatures corresponding to various volume fractions transformed x at different heating rates

x	β ($K\text{min}^{-1}$)					
	2	4	8	16	32	64
0.1	570.4	577.8	586.4	596.4	605.7	618.3
0.4	578.2	586.3	595.1	605.3	616.1	628.7
0.8	586.5	595.1	604.3	614.2	626.4	639.5
0.9	589.4	598.2	607.7	617.4	630.6	643.8

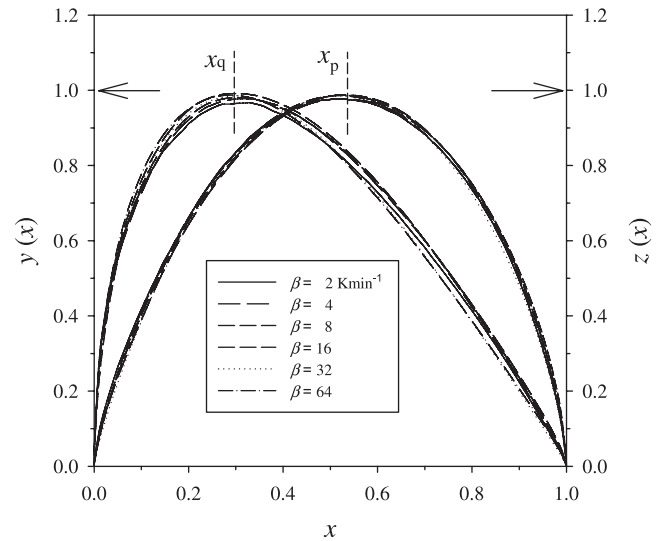


Fig. 4. Plots of normalized $y(x)$ and $z(x)$ functions obtained from experimental data corresponding to the non-isothermal glass–crystal transformation of the $\text{Ge}_{0.13}\text{Sb}_{0.23}\text{Se}_{0.64}$ alloy.

to experimental data of the $\text{Ge}_{0.13}\text{Sb}_{0.23}\text{Se}_{0.64}$ alloy are shown in Fig. 4, which reveals that the quoted model is not fulfilled by the crystallization of the mentioned alloy. It should be noted that the quoted functions show maximum values $x_q = 0.2882$ and $x_p = 0.5206$, according to Fig. 4. These x values are notably different from the corresponding to the JMA model, $x_p = 0.6321$ and $x_q = 0.4204$, in accordance with Eq. (9) and $n = 2.2$. These results seem to confirm again that the kinetic model of normal grain growth, R_n , is the most suitable to describe the crystallization of the alloy studied. In this point, it is interesting to denote that, according to the literature [22], the driving force of grain growth is a force which minimizes the grain boundary energy and which leads to a reduction of the total surface area of the grains. The above-mentioned energy strongly depends on the relative crystal orientation of grains on both sides of the boundary [23,24]. Due to the idea of a strong orientation dependence of the grain boundary energy, there will be a remarkable difference in the properties of grain aggregates as compared with many other cellular structures [25]. It should be noted that, most existing theories on this subject have not considered the crystal orientation effect on grain growth; although during the last two decades some authors [26] have included in their works the crystal orientation dependence of grain boundary energy. The quoted authors have found that the orientation effect does not essentially modify the growth law while it makes the distribution functions for grain sizes and for the number of grain sides broader. They have claimed that the broadness of distribution functions comes from the wetting phenomena of low-energy grain boundaries. Moreover, in accordance with the literature [27], other important

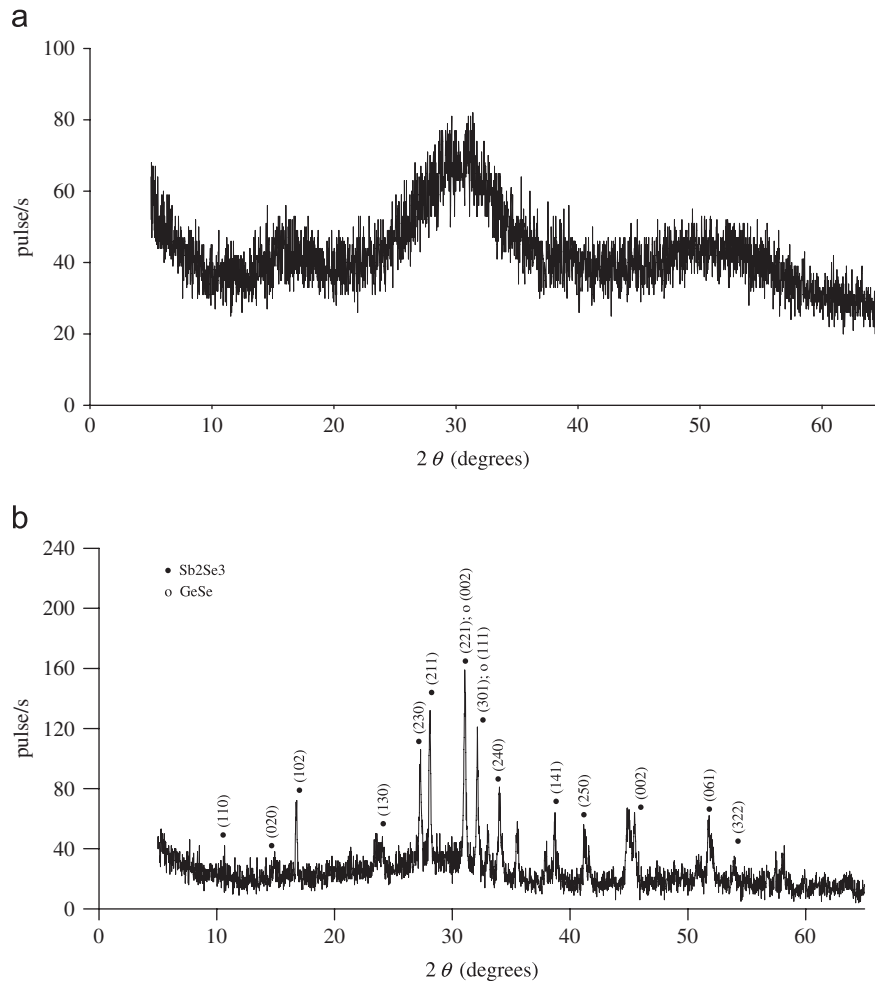


Fig. 5. (A) Diffraction pattern of the $\text{Ge}_{0.13}\text{Sb}_{0.23}\text{Se}_{0.64}$ glassy alloy. (B) Diffraction peaks of crystallized alloy in DSC.

idea is to consider that the mean size of the grains grows proportionally to $t^{1/2}$.

With the aim to explain the probable physical nature of the obtained mechanism, normal grain growth, for the glass–crystal transformation of the $\text{Ge}_{0.13}\text{Sb}_{0.23}\text{Se}_{0.64}$ alloy, we assume the above-mentioned ideas as the essential basis of the quoted physical nature. Thus, it is possible to consider, according to the literature [28], that the grain growth process, probably elapses with accelerating rate. Accordingly, this process is non-linear and the crystal growth rate, u , must depend explicitly on time. This dependence can be expressed as a power law in accordance with the literature [28–30].

Besides, it is interesting to compare the described mechanism in the present work with mechanisms of crystallization of other glasses. In this sense, we have found a large similarity between the quoted mechanism and the crystallization mechanism of the $\text{Ag}_{0.16}\text{As}_{0.42}\text{Se}_{0.42}$ glassy semiconductor, described by us in our paper in press [31]. In the article in press a theoretical method has been developed bearing in mind-oriented nucleation and oriented growth processes. These processes are non-linear and the corresponding rates must depend explicitly on time. In the case of the normal grain growth mechanism obtained in this work, two essential ideas have been already assumed: the crystal orientation effect on grain growth and that the mean size of the grains grows proportionally to $t^{1/2}$. Bearing in mind the quoted ideas it is possible to consider the kinetic model of normal grain growth,

obtained for the $\text{Ge}_{0.13}\text{Sb}_{0.23}\text{Se}_{0.64}$ alloy, as a particular case of the theoretical method developed in the article of the Ref. [31].

5. Identification of the crystalline phases

Taking into account the crystallization exothermal peaks shown by the $\text{Ge}_{0.13}\text{Sb}_{0.23}\text{Se}_{0.64}$ glassy alloy, it is recommended to try to identify the possible phases that crystallize during the thermal treatment applied to the samples by means of adequate XRD measurements. For this purpose, in Fig. 5 we show the most relevant portions of the diffractograms for the as-quenched glass and for the material submitted to the thermal process. Fig. 5A has broad humps characteristic of the amorphous phase of the starting material at diffraction angles (2θ) between 20° and 60° . The diffractogram of the transformed material after the crystallization process (Fig. 5B) suggests the presence of microcrystallites of Sb_2Se_3 and GeSe indicated with ● and ○, respectively, remaining a residual amorphous matrix. The Sb_2Se_3 phase found crystallizes in the orthorhombic system [32] with a unit cell defined by $a = 11.633$, $b = 11.780$ and $c = 3.895$ Å.

6. Conclusions

An integral method has been considered to determine the reaction mechanism model and to calculate the kinetic parameters

by using DSC data, obtained from non-isothermal processes. The assumptions and approximations on which the quoted method is based are the following:

- (i) It is assumed that the glass–crystal transformation rate depends on two independent variables: the volume fraction transformed, x , and the temperature, T .
- (ii) It is supposed that over adequate ranges of x and β values, the analytical forms of $f(x)$ and $K(T)$ functions do not change, and consequently the transformation kinetics does not change.
- (iii) The temperature dependence obeys the Arrhenius relationship.
- (iv) It is carried out the approximation of taking \bar{T} used to calculate the temperature integral, as the average of the considered temperature interval.

The analysis of the kinetic mechanism is based on assumptions (i) and (ii), whilst the calculation of the kinetic parameters may be performed only if the three assumptions and the approximation quoted before, are used together.

The theoretical method considered has been applied to the crystallization kinetics of the $\text{Ge}_{0.13}\text{Sb}_{0.23}\text{Se}_{0.64}$ glassy alloy. According to the study carried out, it is possible to establish that the kinetic model of normal grain growth with $n = 2.2$ is the most suitable to describe the crystallization of the material analyzed. The results obtained for the kinetic parameters: $E = 188.3 \text{ kJ mol}^{-1}$ and $\ln K_0 = 36.7$ are in good agreement with the corresponding values given in the literature for similar alloys. This fact confirms the reliability of the method considered.

Finally, the identification of the crystalline phases has been made by recording the X-ray diffraction pattern of the transformed material. This pattern shows the existence of microcrystallites of Sb_2Se_3 and GeSe in a residual amorphous matrix.

Acknowledgements

The authors are grateful to the Junta de Andalucía (PAI/EXCEL/FQM0654) and the Spanish Ministry of Science and Education (MEC) (Project no. FIS 2005-1409) for their financial supports.

References

- [1] K. Klement Jr., R.H. Willens, P. Duwez, *Nature* 187 (1960) 869.
- [2] A. Inoue, *Mater. Sci. Eng. A* 267 (1999) 171.
- [3] A. Inoue, *Mater. Sci. Eng. A* 375–377 (2004) 16.
- [4] H.E. Kissinger, *Anal. Chem.* 29 (1957) 1702.
- [5] D.W. Henderson, *J. Therm. Anal.* 15 (1979) 325.
- [6] T.J.W. De Bruijin, W.A. De Jong, P.J. Van Den Berg, *Thermochim. Acta* 45 (1981) 315.
- [7] J.R. Frade, *J. Am. Ceram. Soc.* 81 (1998) 2654.
- [8] M. Avrami, *J. Chem. Phys.* 7 (1939) 1103.
- [9] M. Avrami, *J. Chem. Phys.* 8 (1940) 212.
- [10] M. Avrami, *J. Chem. Phys.* 9 (1941) 177.
- [11] H. Yinnon, D.R. Uhlmann, *J. Non-Cryst. Solids* 54 (1983) 253.
- [12] A. Marotta, S. Saiello, F. Branda, A. Buri, *J. Mater. Sci.* 17 (1982) 105.
- [13] A.F. Kozmidis-Petrovic, G.R. Strbac, D.D. Strbac, *J. Non-Cryst. Solids* 353 (2007) 2014.
- [14] D.W. Henderson, *J. Non-Cryst. Solids* 30 (1979) 301.
- [15] C. Popescu, *Thermochim. Acta* 285 (1996) 309.
- [16] J. Málek, *Thermochim. Acta* 267 (1995) 61.
- [17] J.W. Graydon, S.J. Thorpe, D.W. Kirk, *Acta Metall.* 42 (1994) 3163.
- [18] J.W. Cahn, *Acta Metall.* 4 (1956) 572 (*Acta Metall.* 4 (1956) 449).
- [19] J. Vázquez, C. Wagner, P. Villares, R. Jiménez-Garay, *Acta Mater.* 44 (1996) 4807.
- [20] Y.Q. Gao, W. Wang, F.Q. Zheng, X. Liu, *J. Non-Cryst. Solids* 81 (1986) 135.
- [21] J. Vázquez, P.L. López-Aleman, P. Villares, R. Jiménez-Garay, *Mater. Chem. Phys.* 57 (1998) 162.
- [22] T. Nagai, K. Fuchizaki, K. Kawasaki, *Physica A* 204 (1994) 450.
- [23] A.P. Sutton, R.W. Balluffi, *Acta Metall.* 35 (1987) 2177.
- [24] G. Gotstein, F. Schwarzer, *Mater. Sci. Forum* 94–96 (1992) 187.
- [25] J. Stavans, *Rep. Prog. Phys.* 56 (1993) 733.
- [26] Y. Saito, M. Enomoto, *ISIJ Int.* 32 (1992) 267.
- [27] R. Henseler, B. Niethammer, F. Otto, *Int. Series Numer. Math.* 147 (2003) 177.
- [28] R.D. Doherty, K. Kashyap, S. Panchanadeeswaran, *Acta Metall. Mater.* 41 (1993) 3029.
- [29] W.B. Hutchinson, S. Jonsson, L. Ryde, *Scripta Metall.* 23 (1989) 671.
- [30] C. Necker, R.D. Doherty, A.D. Rollet, in: *Ninth International Conference on Textures*, Avignon, 1990, *Texture Microstructure*, France, 1991, vol. 635, pp. 14–18.
- [31] J.L. Cárdenas, et al., *J. Alloys Compd.* (2008).
- [32] S.A. Dembovski, *Russ. J. Inorg. Chem. (Engl. Transl.)* 8 (1963) 798.